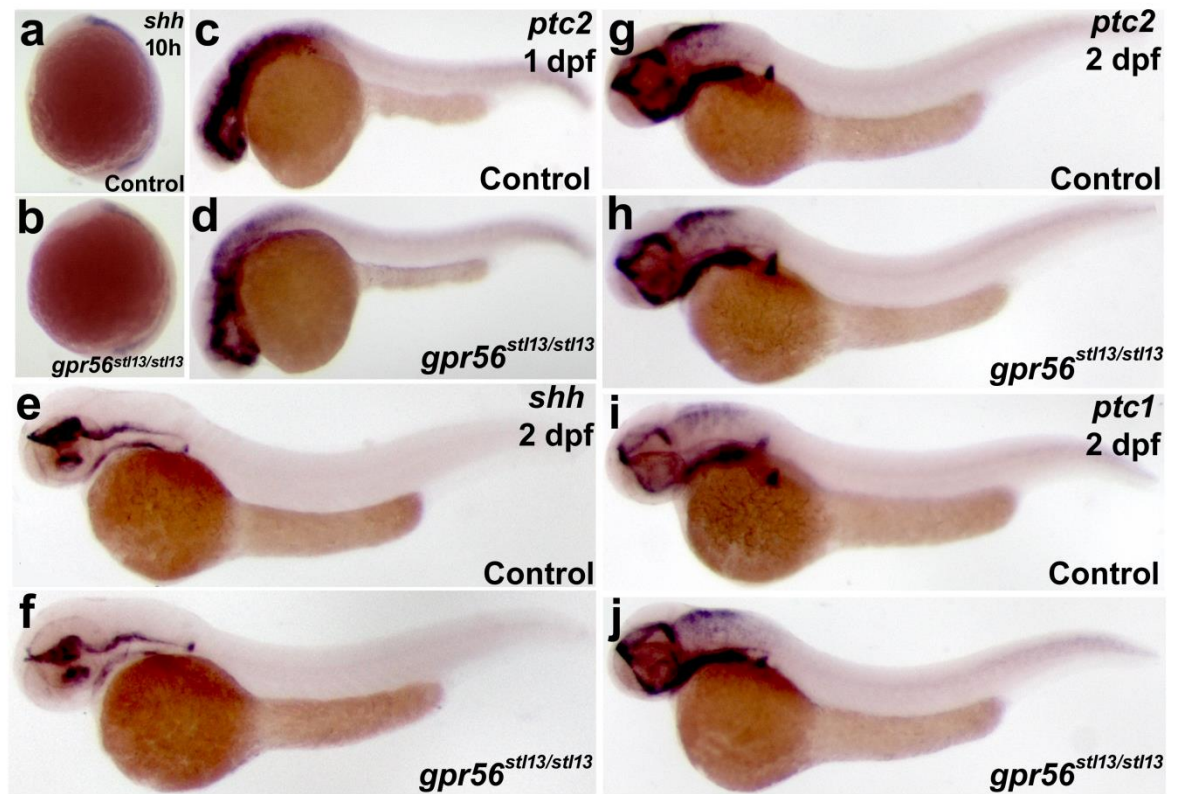


Supplementary Figure 1



Supplementary Figure 1. *gpr56* staining via WISH is specific and time-dependent. (a) An embryo showing *gpr56* WISH staining at 5 dpf (three technical replicates). (b) Higher magnification of anterior region. (c) An embryo showing *gpr56* sense control WISH staining at 3 dpf (two technical replicates). Lateral views shown with anterior to the left and posterior to the right in all images.

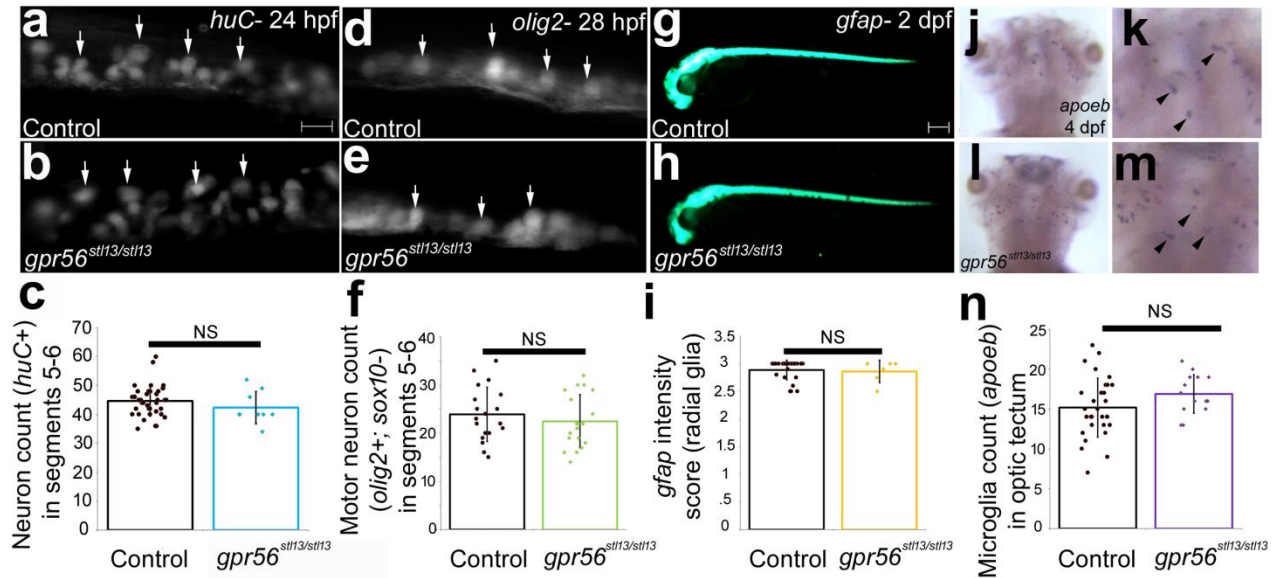
Supplementary Figure 2



Supplementary Figure 2. Dorsal-ventral patterning is not affected in *gpr56* mutants.

Representative control (a, c, e, g, i) versus *gpr56*^{stl13/stl13} mutant (b, d, f, h, j) embryos stained for *shh* (control: *N*=14/18, *gpr56*^{stl13/stl13}: *N*=5/5 at 10 hours (10h); control: *N*=13/17, *gpr56*^{stl13/stl13}: *N*=5/7 at 2 dpf), *ptc1* (control: *N*=14/14, *gpr56*^{stl13/stl13}: *N*=5/5 at 2 dpf), or *ptc2* (control: *N*=14/17, *gpr56*^{stl13/stl13}: *N*=5/6 at 1 dpf; control: *N*=12/13, *gpr56*^{stl13/stl13}: *N*=7/7) by WISH. All images are representative of two technical replicates.

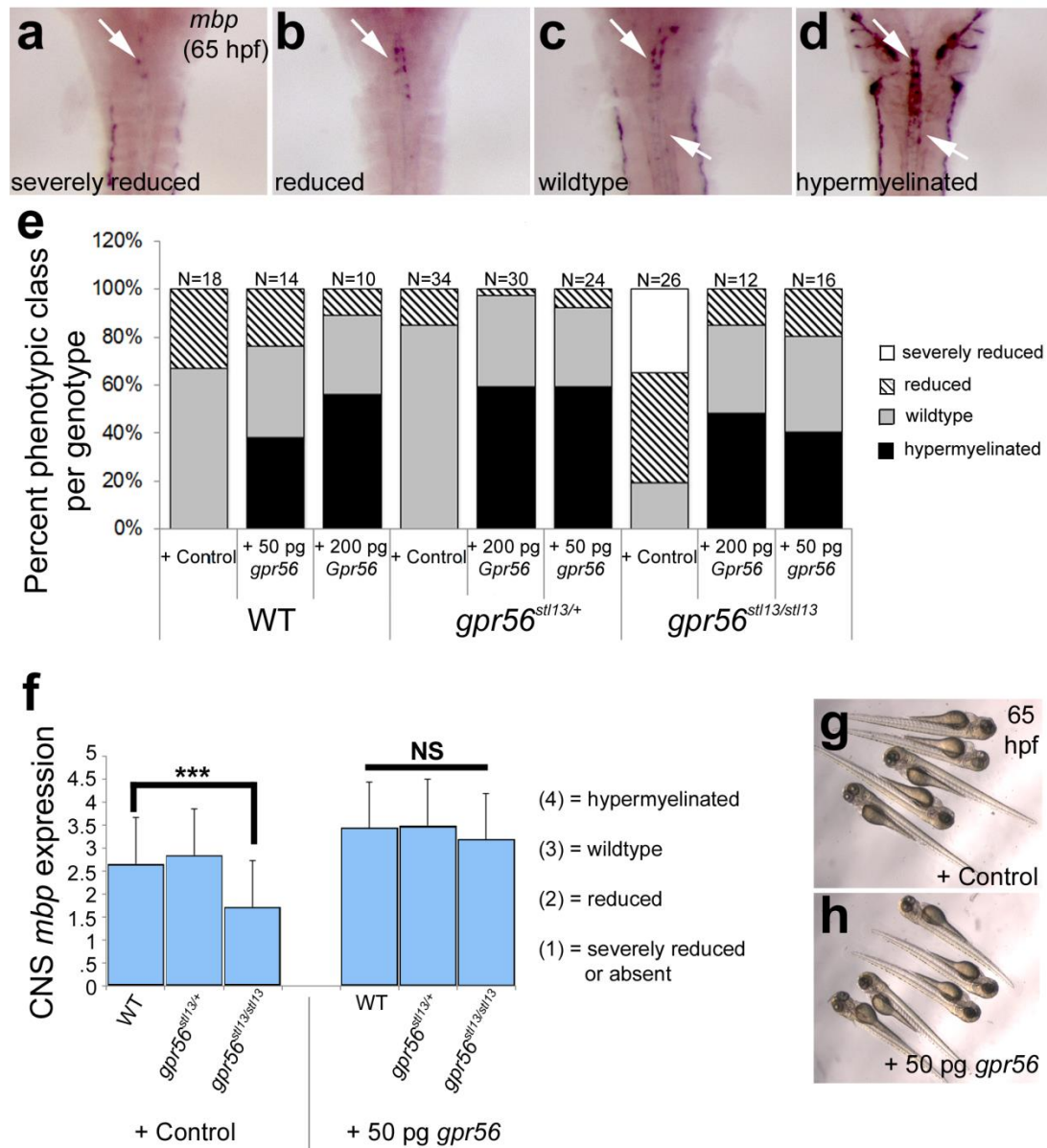
Supplementary Figure 3



Supplementary Figure 3. Numbers of neurons, radial glia, and microglia are unchanged in *gpr56* mutants. (a-b) Representative fluorescent images of the control (*gpr56*^{+/+} and *gpr56*^{stl13/+}, a) and *gpr56*^{stl13/stl13} (b) larvae at 24 hpf expressing *tg(HuC:Kaede)* to mark all neurons (white arrows). (c) We found no significant difference in total neuron number in control (N= 39) versus mutant (N=9) larvae ($p < .29$, Student's t-test). (d-e) Representative fluorescent images of control (*gpr56*^{stl13/+}, d) and *gpr56*^{stl13/stl13} (e) larvae at 28 hpf expressing *tg(olig2:DsRed)* to mark motor neurons (white arrows). (f) Quantification of *olig2*+/; *sox10*- motor neuron number (white arrows) in control (N=20) and *gpr56*^{stl13/stl13} (N=19) larvae ($p < .44$, Student's t-test). (g-h) Representative fluorescent images of control (*gpr56*^{+/+} and *gpr56*^{stl13/+}, g) and *gpr56*^{stl13/stl13} (h) larvae at 48 hpf expressing *tg(gfap:gfp)* to mark radial glia. (i) Quantification of average fluorescence intensity in mutant (N=6) and control larvae (N=29, $p < .75$, Student's t-test). (j-k) Representative WISH images of control (*gpr56*^{+/+} and *gpr56*^{stl13/+}, j) and *gpr56*^{stl13/stl13} (l) larvae at 4 dpf stained for *apoeb* to mark microglia (black arrowheads). (n) Quantification of microglia number in mutants (N=15) and controls (N=31, $p < .07$, Student's t-test). k and m are higher magnification images of

j and **l**, respectively. (**a-f**) All images and quantification thereof were taken from segments 5-6 for consistency. (**a-h**) Lateral views are shown, anterior to the left, dorsal is up. (**a-e**) Scale bar, 50 μm . (**g-h**) Scale bar, 250 μm . (**j-m**) Dorsal view shown, anterior is up. Two technical replicates were performed for each molecular marker. Error bars are shown as \pm s.d. NS, not significant.

Supplementary Figure 4

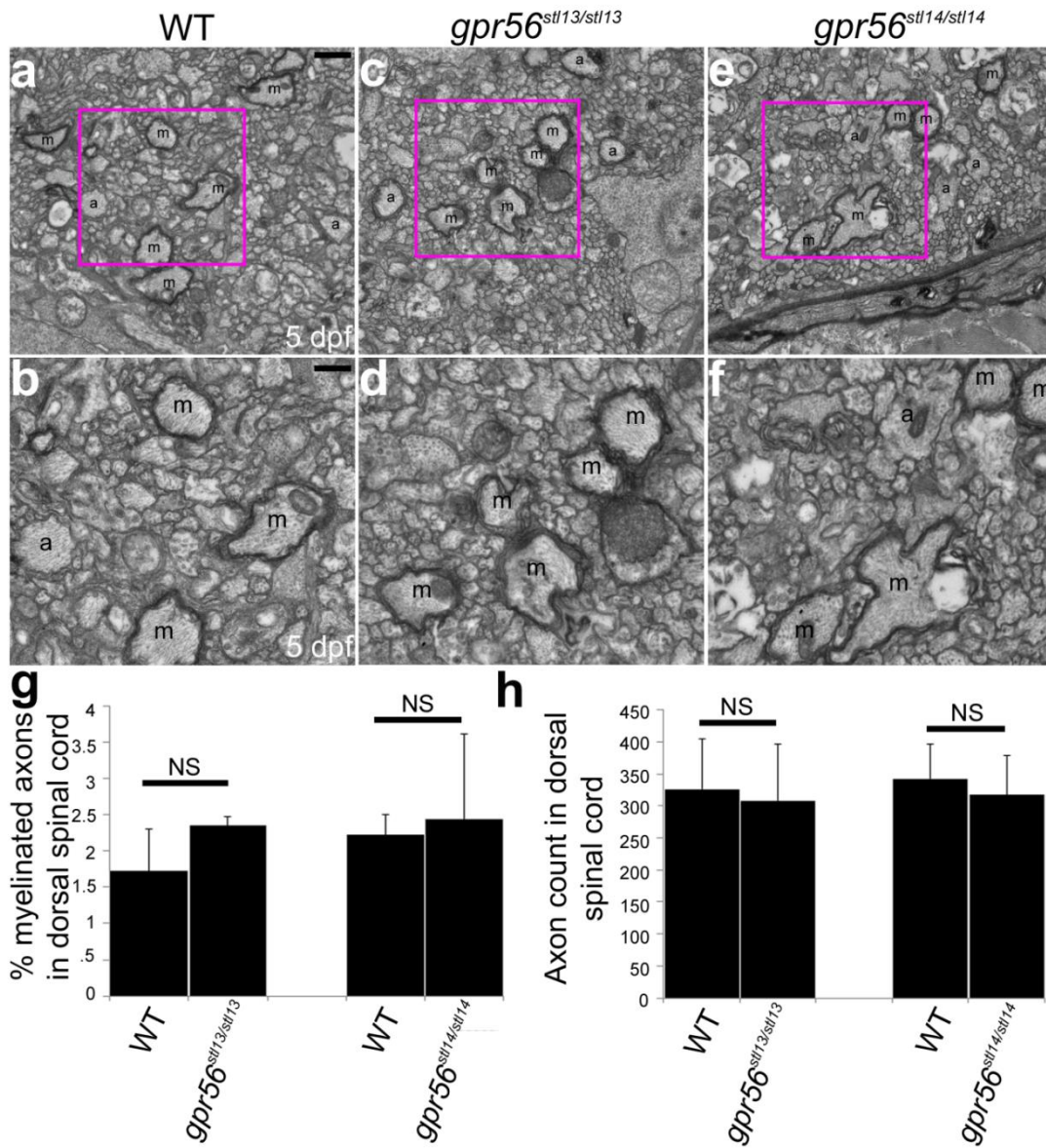


Supplementary Figure 4. Overexpression of *gpr56* suppresses *mbp* deficits in *gpr56*

mutants. (a-d) Overexpression (OE) of wildtype (WT) mouse (200 pg) or zebrafish (50 pg) *Gpr56* synthetic mRNA or phenol red control yielded embryos with (a) strongly reduced, (b) reduced, (c) wildtype, (d) or hypermyelinated CNS *mbp* expression at 65 hpf by WISH (dorsal

views shown, anterior is up). Larvae were given a score of 1-4 based on their *mbp* expression: 1=strongly reduced, 2=reduced, 3=wildtype, 4=hypermyelinated. (e) Phenotypic distribution of WT, *gpr56*^{+/-}, and *gpr56*^{stil13/stil13} embryos separated by treatment. (f) Quantification of CNS *mbp* score separated by genotype and treatment (control WT versus control mutant: $p < .0004$, Student's t-test; *gpr56*-injected WT versus *gpr56*-injected mutants: $p < .42$, Student's t-test). (g-h) All analyzed *gpr56* injected embryos were morphologically normal. Two technical replicates were performed. Error bars are shown as + s.d. NS, not significant.

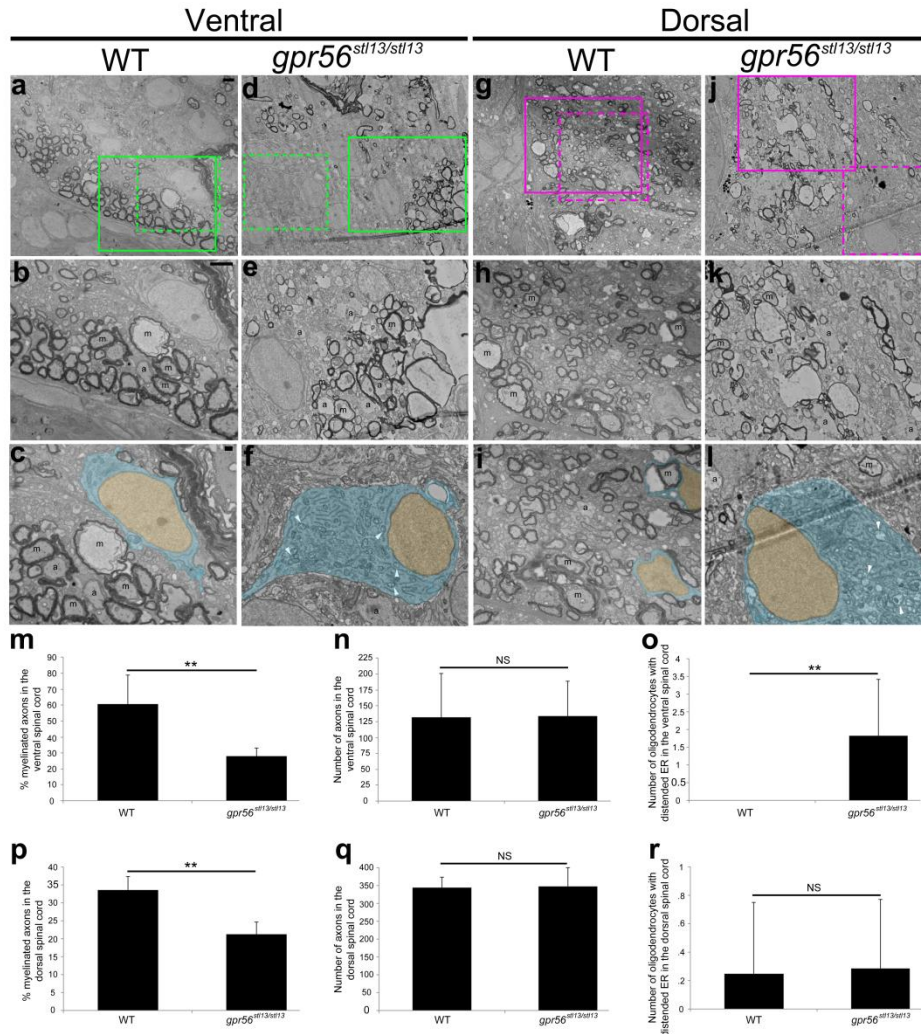
Supplementary Figure 5



Supplementary Figure 5. Oligodendrocyte myelination is unaffected in the dorsal spinal cord of *gpr56* mutants at 5 dpf. (a-f) Representative TEM images from the dorsal spinal cord of WT (a-b), *gpr56*^{stl13/stl13} (c-d) and *gpr56*^{stl14/stl14} (e-f) mutant larvae. Images in (b,d,f) show higher magnifications of the magenta, boxed-in regions of (a,c,e). Quantification of the percent of myelinated axons (g, WT versus *gpr56*^{stl13/stl13}: $p < .2$, Student's t-test; WT versus *gpr56*^{stl14/stl14}: $p < .78$, Student's t-test) and the total number of axons (h, WT versus

gpr56^{stl13/stl13}: $p < .82$, Student's t-test; WT versus *gpr56*^{stl14/stl14}: $p < .62$, Student's t-test) in the dorsal spinal cord of *gpr56*^{stl13/stl13} (**c-d**, $N=5$) and *gpr56*^{stl14/stl14} (**e-f**, $N=4$) mutants and controls (**a-b**, $N=6$) at 5 dpf. (**a,c,e**) Scale bar, 1 μm . (**b,d,f**) Scale bar, 500 nm. (**g-h**) Quantification performed on a stereotyped 14 μm^2 region (see Fig. 3b) in the ventral spinal cord. m, myelinated axon. a, large unmyelinated axon. Two technical replicates were performed. Error bars are shown as + s.d. NS, not significant.

Supplementary Figure 6

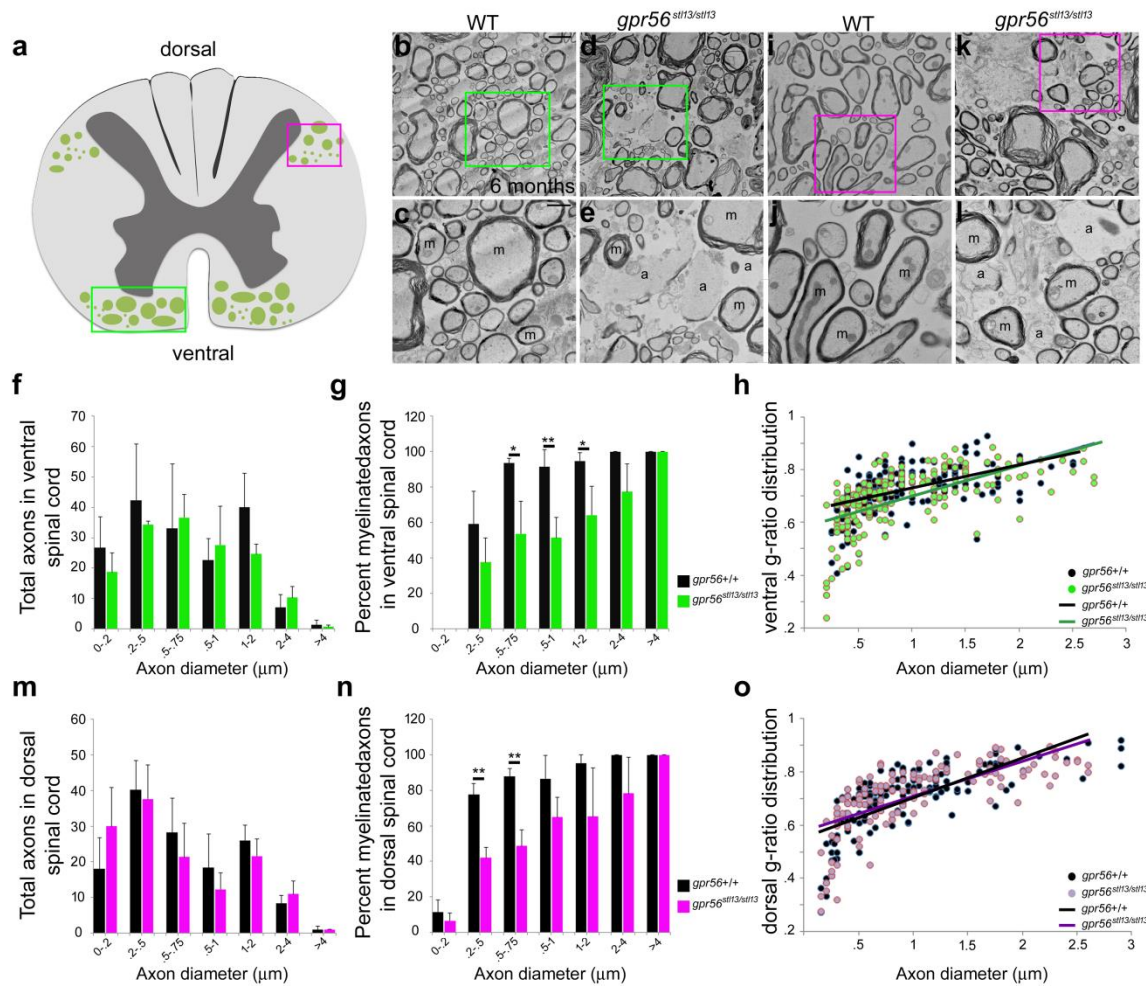


Supplementary Figure 6. *gpr56* mutant juveniles show CNS hypomyelination. (a-f)

Representative TEM images of cross-sections through the ventral spinal cord of WT controls (a-c, $N=2$) and *gpr56^{stl13/stl13}* mutant siblings (d-f, $N=4$) at 21 dpf. (g-l) Representative TEM images of cross-sections through the dorsal spinal cord of WT controls (g-i, $N=2$) and *gpr56^{stl13/stl13}* mutants (j-l, $N=4$) at 21 dpf. (m) Quantification of the percent of myelinated axons ($p<.007$, Student's t-test), and (n) axon number in the ventral spinal cord ($p<.96$, Student's t-test). (o) Quantification of the number of oligodendrocytes with swollen endoplasmic reticulum (ER, oligodendrocyte nuclei pseudocolored orange, cytoplasm pseudocolored blue) in (f) *gpr56^{stl13/stl13}*

mutants and **(c)** controls ($p < .003$, Student's t-test). **(p)** Quantification of the percent of myelinated axons in of the dorsal spinal cord $gpr56^{stl13/stl13}$ mutants and control siblings ($p < .002$, Student's t-test). **(q)** Quantification of axon number ($p < .89$, Student's t-test) and the number of oligodendrocytes with distended ER **(r)** in the dorsal spinal cord of **(l)** $gpr56^{stl13/stl13}$ mutants and **(i)** controls ($p < .92$, Student's t-test). Quantifications were performed on stereotyped 20 μm regions of the dorsal and ventral spinal cord (diagram in Fig. 3b). Solid boxed in regions in panels **a,d,g,j** are magnified and shown in panels **b,e,h,k**, respectively. Dashed boxed in panels **a,d,g,j** are magnified in **c,f,i,l**. Examples of myelinated axons are marked with the letter "m", and examples of unmyelinated axons of similar caliber are marked with the letter "a". Scale bar for **a-b, d-e, g-h, j-k**, 2 μm . Scale bar for **c,f,i,l**, 500 nm. One technical replicate was performed. Error bars are shown as + s.d. NS, not significant.

Supplementary Figure 7

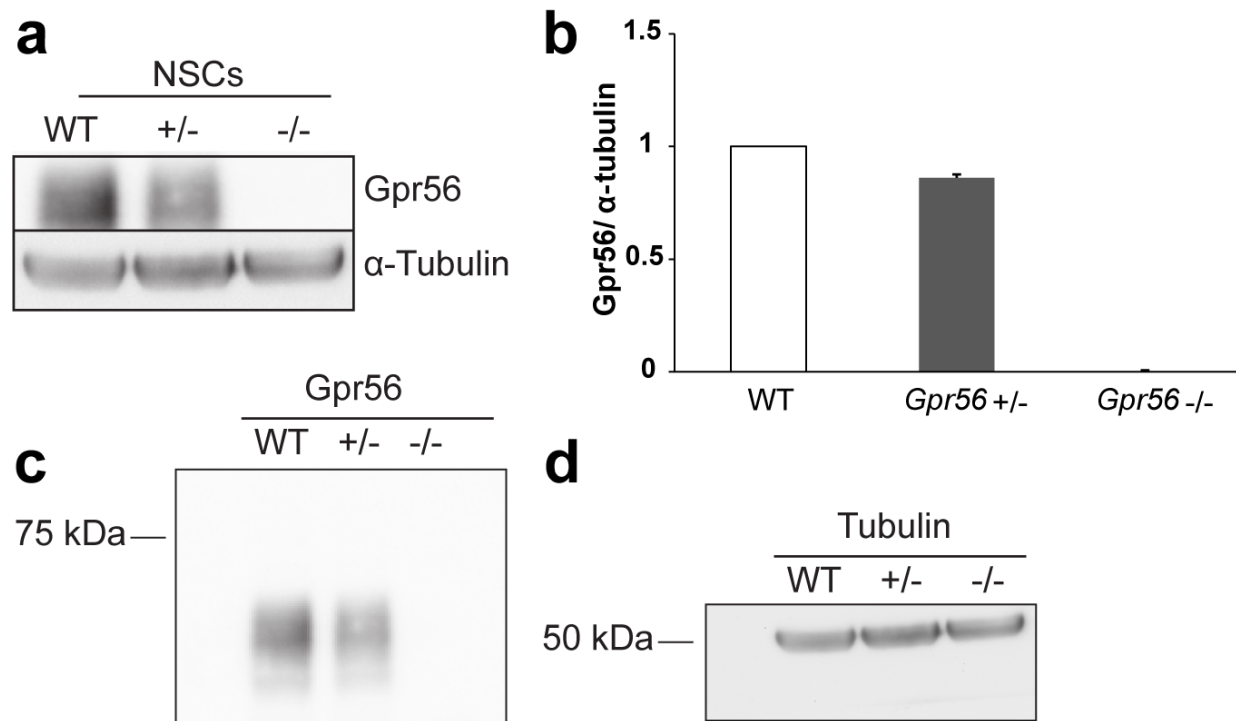


Supplementary Figure 7. *gpr56* mutants exhibit prolonged CNS hypomyelination.

(a) Schematic representation of a cross-section through the adult zebrafish spinal cord. Grey matter in dark grey, white matter in light grey. Myelinated axons are represented by green ovals, and quantified regions are boxed in magenta for the dorsal spinal cord and green for the ventral spinal cord. **(b-c, g-h)** Representative TEM images from the spinal cord of WT (**b-c, i-j**, $N=3$) and $gpr56^{stl13/stl13}$ mutant adults (**d-e, k-l**, $N=4$) at 6 months of age. **(f)** Quantification of total axon number and **(g)** the percent of myelinated axons in the ventral spinal cord of $gpr56^{stl13/stl13}$ mutants and controls separated by axon diameter. **(f)** P-values for axon number by diameter:

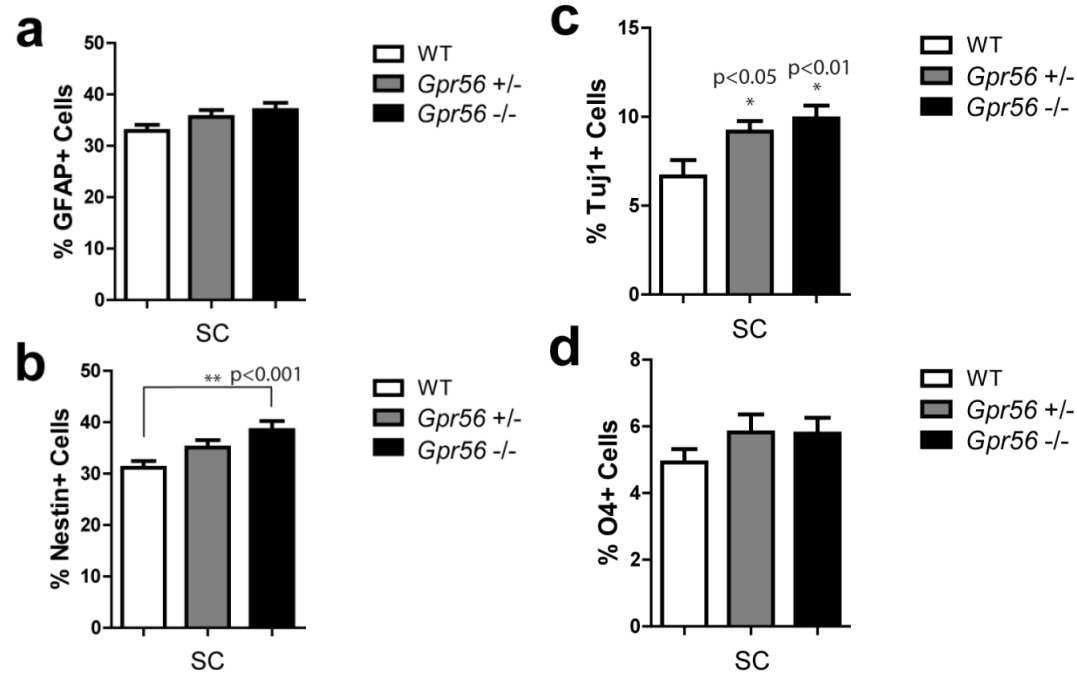
2µm: $p < .33$; .2-.5µm: $p < .54$; .5-.75 µm: $p < .81$; .75-1 µm: $p < .60$; 1-2 µm: $p < .14$; 2-4 µm: $p < .37$; >4 µm: $p < .54$, Student's t-test. **(g)** P-values for percent myelinated axons by diameter: 0-.2µm (N/A), .2-.5 µm ($p < .17$), .5-.75 µm ($p < .021$), .75-1 µm ($p < .005$), 1-2 µm ($p < .029$), 2-4µm ($p < .07$), >4 µm (N/A), Student's t-test. **(h)** Quantification of g-ratio (diameter of axon/diameter of myelinated fiber) in the ventral spinal cord of *gpr56^{stl13/stl13}* mutants and controls.(linear regression analysis). **(m)** Quantification of total axon number and **(n)** the percent of myelinated axons in the dorsal spinal cord of *gpr56^{stl13/stl13}* mutants and controls separated by diameter. **(m)** P-values for total axon number by diameter: 0-.2µm ($p < .22$), .2-.5µm ($p < .73$), .5-.75 µm ($p < .42$), .75-1 µm ($p < .40$), 1-2 µm ($p < .31$), 2-4 µm ($p < .36$), >4 µm ($p = 1$), Student's t-test. **(n)** P-values for the percent myelinated axons by diameter: 0-.2µm ($p < .37$), .2-.5 µm ($p < .003$), and .5-75 µm($p < .008$), .75-1 µm ($p < .10$), 1-2 µm ($p < .20$), 2-4 µm ($p < .21$), >4 µm (N/A), Student's t-test. **(o)** Quantification of g-ratios (diameter of axon/diameter of myelinated fiber) in the dorsal spinal cord of *gpr56^{stl13/stl13}* mutants and controls (linear regression analysis). **(b,d,i,k)** Scale bar, 2 µm. **(c,e,j,l)** Scale bar, 1 µm. Panels **c,e,j,l** are magnified images of the boxed-in regions of panels **b,d,i,k**. **(b-e, i-l)** Quantification performed on stereotyped 17 µm² regions **(a)** of the ventral and dorsal spinal cord. Two technical replicates were performed. Error bars are shown as \pm s.d.

Supplementary Figure 8



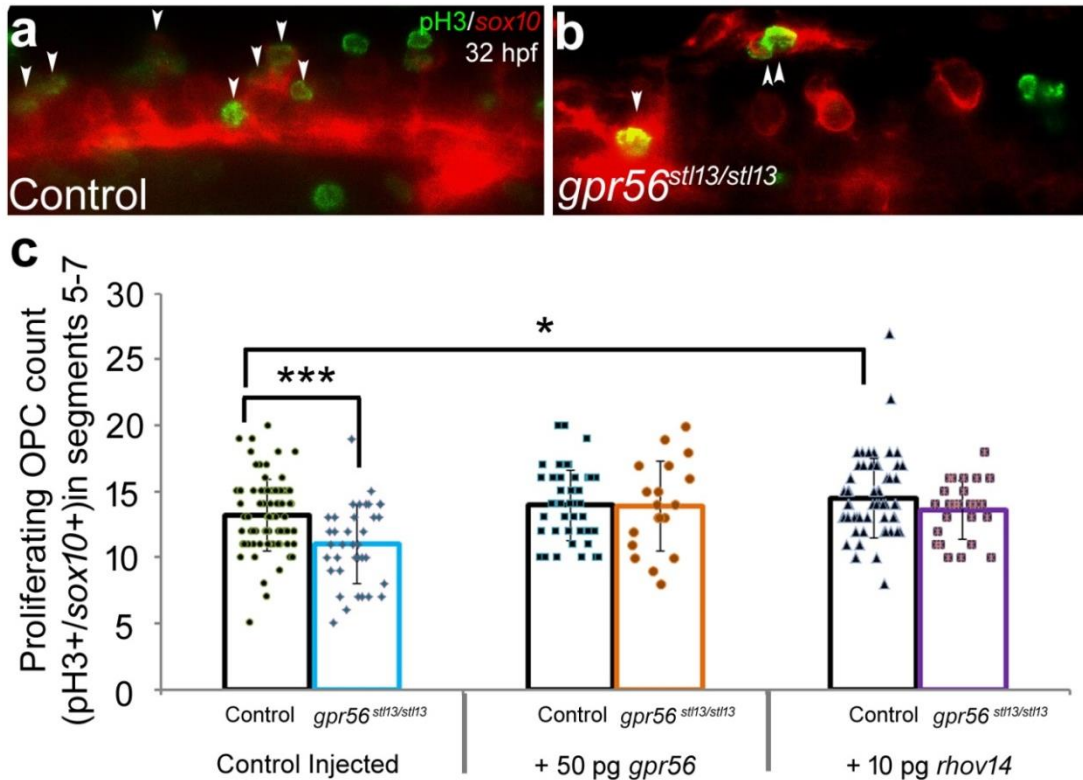
Supplementary Figure 8. Gpr56 is present in mouse neurospheres. (a) Western blot showing Gpr56 protein levels in neurospheres harvested from the subventricular zones of *Gpr56* *+/+* (WT, *N*=4), *Gpr56* *+/-* (*N*=4), and *Gpr56* *-/-* (*N*=3) P3 animals. α-Tubulin was used as a loading control. (b) Relative Gpr56 levels per genotype using western blot analysis calculated by averaging Gpr56 chemiluminescence intensity for each genotype from two separate litters. (c) Full western showing Gpr56 protein levels and (d) full western blot showing Tubulin protein levels used to generate panel a. Approximate expected protein masses: Gpr56^N: 60 kDa, Tubulin: 50 kDa. Two technical replicates were performed. Error bars are shown as + s.d.

Supplementary Figure 9



Supplementary Figure 9. Loss of *Gpr56* in the SC biases neural stem cell differentiation to neurons. Quantification of the percent of (a) GFAP+ astrocytes, (b) Nestin+ neural progenitors, (c) Tuj1+ neurons and (d) O4+ oligodendrocytes per field of view differentiated from neurospheres harvested from WT ($N=3$), *Gpr56*^{+/-} ($N=4$) and *Gpr56*^{-/-} ($N=5$) animals at P3. Statistical test employed: two-way ANOVA. Two technical replicates were performed. Error bars are shown as + s.d.

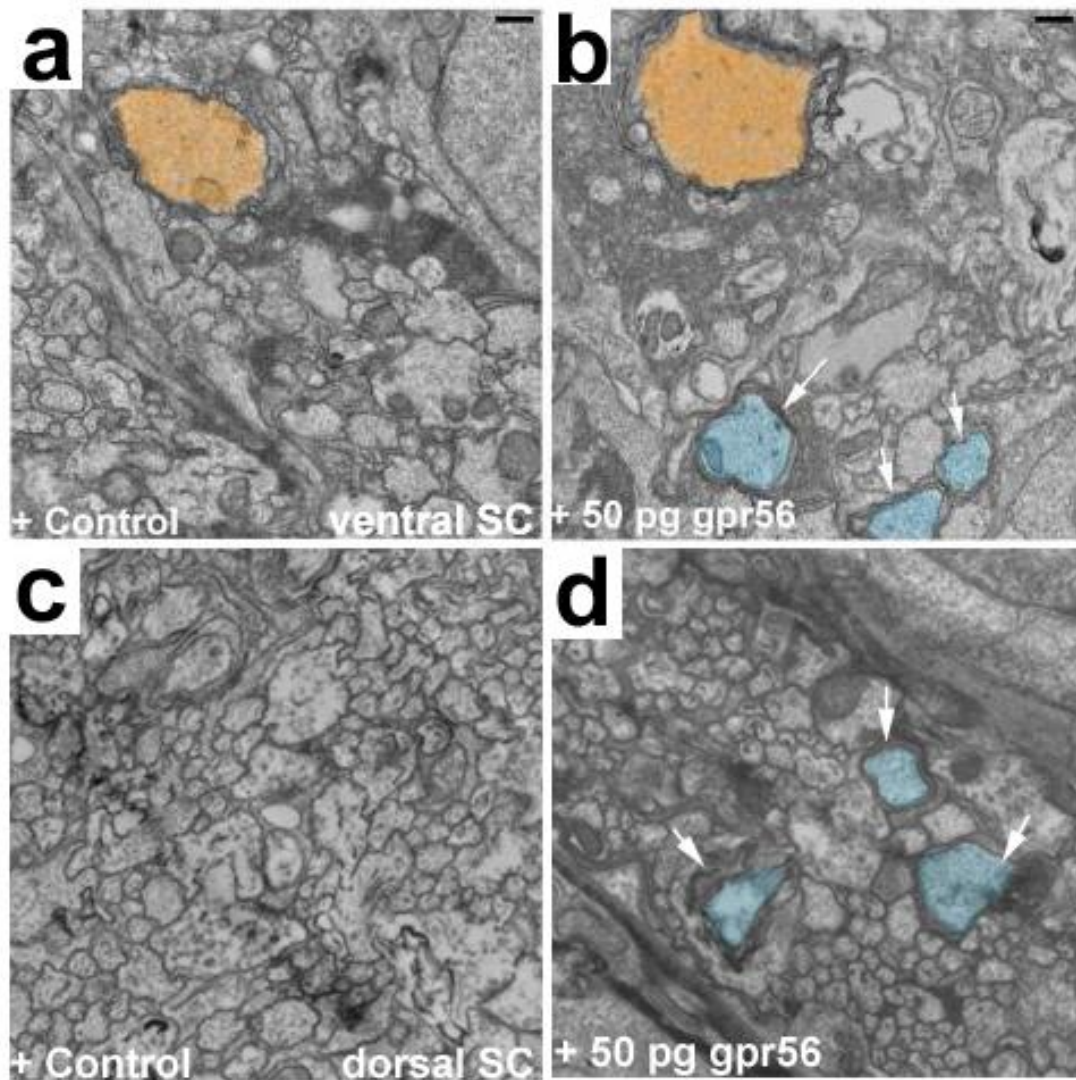
Supplementary Figure 10



Supplementary Figure 10. Overexpression of *gpr56* or constitutively active *rhoa* suppresses *gpr56^{stl13/stl13}* OPC proliferation defects. Representative fluorescent images of the spinal cord from segments 5-7 of phenol-red injected (a) control (*gpr56^{+/+}* and *gpr56^{stl13/+}*, $N=78$) and (b) *gpr56^{stl13/stl13}* mutant ($N=37$) embryos at 32 hpf. Embryos expressing *tg(sox10 (-7.2):mRFP)* were fixed and stained with pH3 to assay proliferation. Scale, 50 μ m. (c) Quantification of the number of proliferating OPCs (*gpr56^{stl13/stl13}* mutants versus controls) in control injected embryos ($p<.0003$, Student's t-test), *gpr56* injected embryos ($p<.92$, Student's t-test) and in *rhov14* injected embryos ($p<.15$, Student's t-test). Quantification of OPC proliferation in *gpr56^{+/+}* and *gpr56^{+/+}* controls in the presence of excess *rhoa* compared to control injected ($p<.013$, Student's t-test). *gpr56*-injected control embryos: $N=49$. *gpr56*-injected mutant embryos: $N=19$. *rhov14*-

injected control embryos: $N=62$. *rhov14*-injected mutant embryos: $N=25$. Two technical replicates were performed. Error bars are shown as \pm s.d.

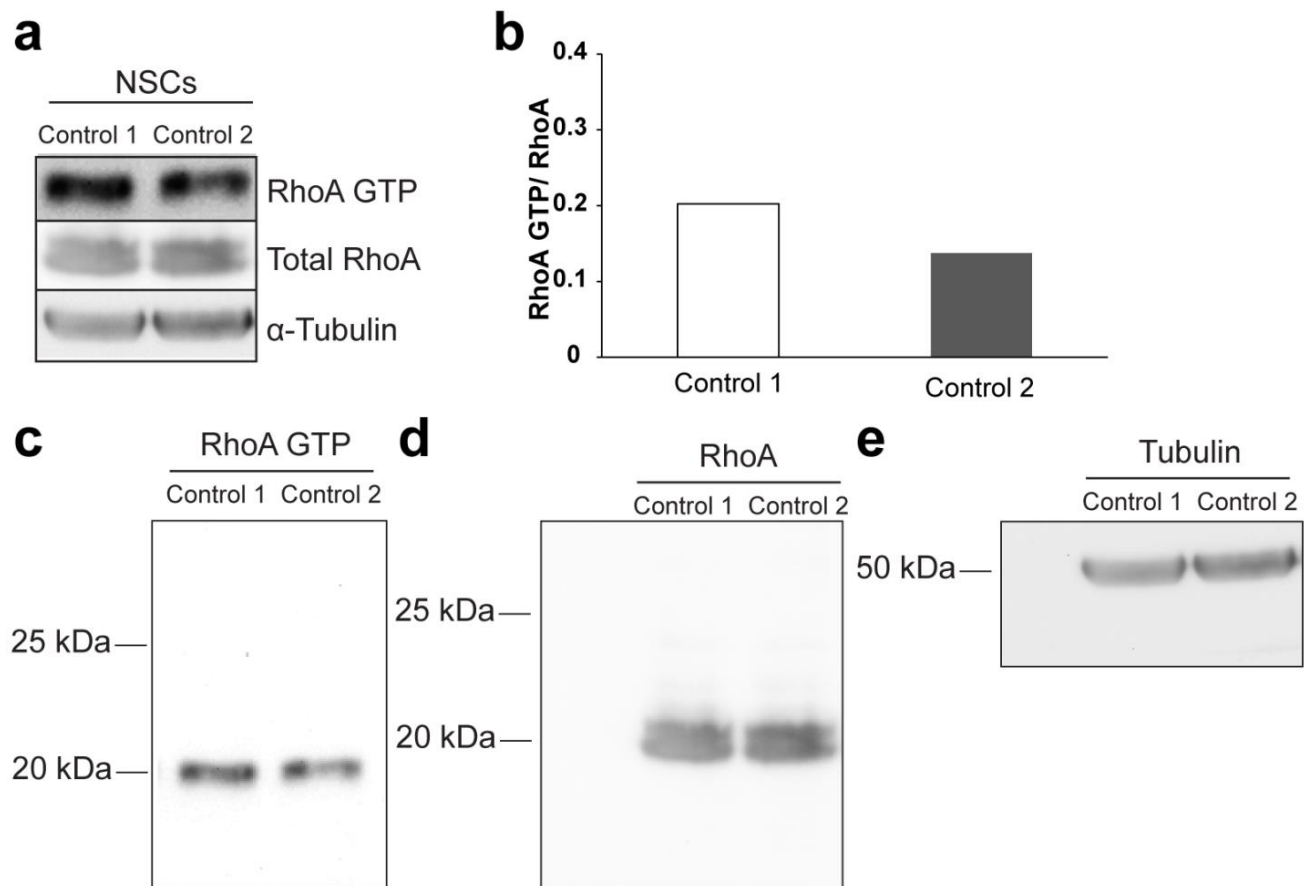
Supplementary Figure 11



Supplementary Figure 11. Overexpression of *gpr56* affects oligodendrocyte myelination.

(a-d) Representative images of ventral (a-b) and dorsal (c-d) spinal cord cross-sections from 2.5 dpf WT embryos injected with control (a, c) or 50 pg *gpr56* synthetic mRNA (b, d). Additional myelinated axons (blue pseudocolor, white arrows) were observed in the ventral spinal cord of 2/4 and 1/4 *gpr56* injected embryos compared to controls in the ventral and dorsal spinal cord (SC), respectively. Large caliber, Mauthner axon pseudocolored orange. Scale, 500 nm. Two technical replicates were performed.

Supplementary Figure 12



Supplementary Figure 12. RhoA is present and active in mouse neurospheres. (a) Western blot showing Total RhoA and active RhoA (RhoA GTP) levels in neurospheres harvested from the subventricular zone of control (WT and *Gpr56* +/-, *N*=3) animals at P3. α-Tubulin was used as a loading control. (b) Quantification of (a) showing the proportion of active RhoA to total RhoA in each control sample. (c-e) Full western blots showing RhoA GTP (c), total RhoA (d) and Tubulin (e) protein levels used to generate panel a. Approximate expected protein masses: RhoA-GTP: 20 kDa; RhoA: 20 kDa; Tubulin: 50 kDa. Two technical replicates were performed.